SUPPLEMENT

EXPLAINING EXTREME EVENTS OF 2016 FROM A CLIMATE PERSPECTIVE

Editors
Stephanie C. Herring, Nikolaos Christidis, Andrew Hoell, James P. Kossin,
Carl J. Schreck III, and Peter A. Stott

Special Electronic Supplement to the
Bulletin of the American Meteorological Society
Vol. 99, No. 1, January 2018

Cover credits:
©The Ocean Agency / XL Catlin Seaview Survey / Chrisophe Bailhache—A panoramic image of coral bleaching at Lizard Island on the Great Barrier Reef, captured by The Ocean Agency / XL Catlin Seaview Survey / Christophe Bailhache in March 2016.

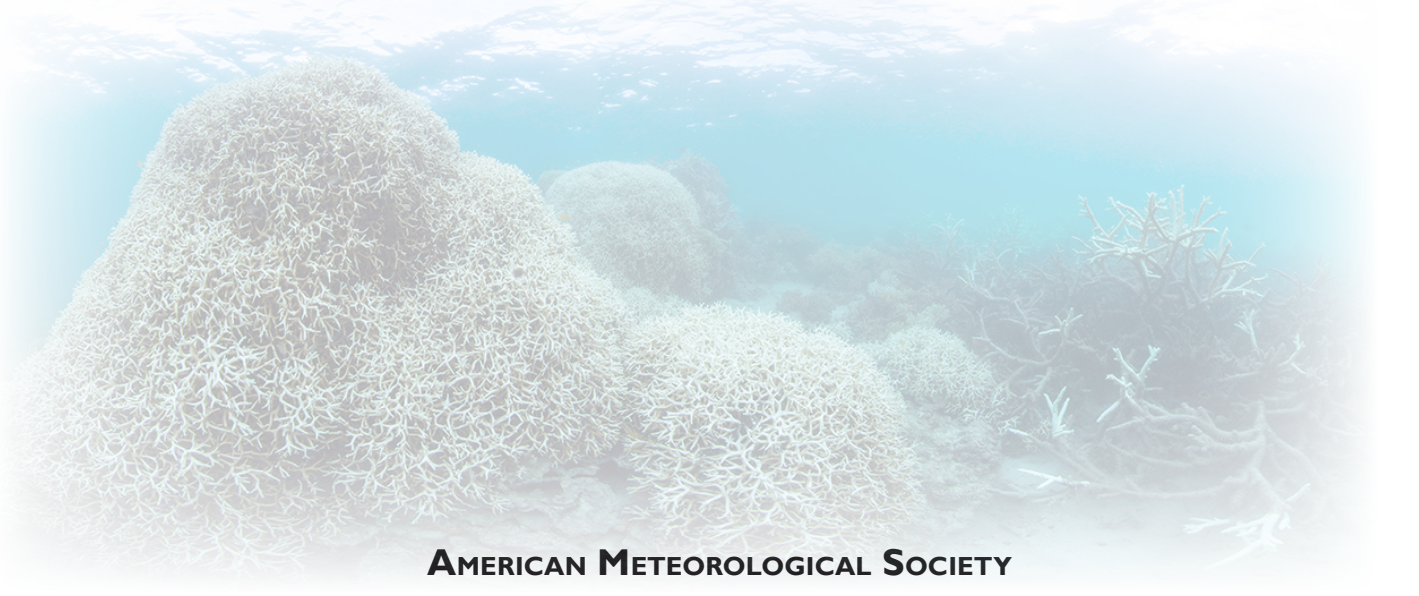

AMERICAN METEOROLOGICAL SOCIETY

ES3. CMIP5 MODEL-BASED ASSESSMENT OF ANTHROPOGENIC INFLUENCE ON RECORD GLOBAL WARMTH DURING 2016

Thomas R. Knutson, Jonghun Kam, Fanrong Zeng, and Andrew T. Wittenberg

This document is a supplement to "CMIP5 model-based assessment of anthropogenic influence on record global warmth during 2016," by Thomas R. Knutson, Jonghun Kam, Fanrong Zeng, and Andrew T. Wittenberg (*Bull. Amer. Meteor. Soc.*, **99** (1), S11–S15) • ©2018 American Meteorological Society • DOI:10.1175/BAMS-D-17-0104.2

S.1. CMIP5 model characteristics.

Table ES3.1 lists the CMIP5 (Taylor et al. 2012) models used, ensemble sizes, and ensemble-mean responses for 2016. All-Forcing run time series were extended from 2006 to 2016 using RCP8.5 scenario ensemble members, reusing RCP8.5 ensemble member 1 for cases where no matching RCP8.5 member was available for an All-Forcing ensemble member. At least two ensemble members were required to estimate an ensemble mean for a scenario. Since the CMIP5 Natural Forcing runs end in 2005 or 2012, one must extrapolate to estimate a Natural-Forced response for 2016. For our analysis, we estimated the 2016 response as the time-averaged response from 2001 to the end of each model's run (2005 or 2012; see main text Fig. 3.1b). This may exclude some recent natural cooling influences due to volcanic aerosol not included in the CMIP5 runs post-2005 (Ridley et al. 2014).

The available Natural Forcing-Only and All Forcing simulations (e.g., main text Figs. 3.1a,b) provide only a limited sample of modeled internal variability, with relatively few ensemble members per model (Table ES3.1). We therefore use the long pre-industrial CMIP5 Control runs in our study to better sample the possible role of internal climate variability in the 2016 event. For this, we are assuming that the Control runs' global temperature variability remains representative of real-world internal variability through 2016. The adequacy of the CMIP5 climate model simulations of internal variability for detection and attribution in general have been assessed previously (e.g., IPCC 2013; Knutson et al. 2013, 2016). These studies suggest that it is very unlikely that models *underestimate* internal multidecadal variability of the climate system by enough to affect century-scale trend detections such as inferred from main text Figs. 3.1b,c. The internal variability estimate for the real world for 2016 is estimated as the GISTEMP observed anomaly (relative to 1881–1920) minus the All-Forcing ensemble mean for 2016.

The individual CMIP5 models are assessed for consistency with observations for 2011 (a relatively cool recent year) and 2016 (new record warm year) global anomalies. We used both a relatively recent cool year and the new record warm year (2016) for our dual-year consistency test to reduce the bias that would be created by using only the recent warm year as a screening criterion. To be consistent, observed values for both 2011 and 2016 were required to fall within a model-simulated range defined by a given model's All-Forcing mean response for that year bracketed by the range of annual means from its control run. The results of this dual-year consistency test are also depicted in Table ES3.1.

S.2. Methodological details for main text Fig. 3.1.

The observed data websites and references are: GISTEMP (https://data.giss.nasa.gov/gistemp/; Hansen et al. 2010); HadCRUTT4.5 (http://www.metoffice.gov.uk/hadobs/hadcrut4/data/current/download.html; Morice et al. 2012); and NOAA

Table ES3.1. List of CMIP5 models used in the study, including ensemble sizes for All-Forcing, RCP8.5 extension to 2016, and Natural Forcing scenarios; end year of Natural Forcing runs; and control run lengths. The seven models with at least two ensemble members for All-Forcing, RCP8.5 extension, and Natural-Forcing are highlighted in bold. Models that pass the consistency test (see text) are denoted by underlined estimates. Ensemble mean forced responses for models with adequate number of ensemble members are shown (in °C, relative to 1881–1920) for the Jan–Dec 2016 annual mean for All Forcing, Natural Forcing, and Anthropogenic Forcing (All-Forcing minus Natural-Forcing), with the internal variability estimated as a residual (Observed minus All-Forcing).

ID	Model Name	# Runs: All-Forcing; RCP8.5 extension	# Runs: Natural Forcing	End Year: Natural Forcing	# Years: Control Run	All-Forcing Ens. Mean, °C	Natural Forcing Ens. Mean, °C	Anthro. Forcing Ens. Mean, °C	Internal Variab. Residual Est., °C
	ACCESS1-0	1; 1	—	—	500	—	—	—	—
	ACCESS1-3	3; 1	—	—	500	—	—	—	—
	BCC-CSM1	3; 1	1	2012	500	—	—	—	—
	BNU-ESM	1; 1	1	2005	559	—	—	—	—
	CanESM2	**5; 5**	**5**	2012	996	+1.54	+0.08	+1.46	−0.27
	CCSM4	6; 5	1	2005	501	+1.45	—	—	−0.17
	CESM1-BGC	1; 1	—	—	500	—	—	—	—
	CESM1-CAM5	**3; 3**	**3**	2005	319	+1.02	+0.17	+0.85	0.26
	CMCC-CM	1; 1	—	—	330	—	—	—	—
0	CMCC-CMS	1; 1	—	—	500	—	—	—	—
1	CNRM-CM5	1; 1	1	2012	850	—	—	—	—
2	**CSIRO-Mk3-6-0**	**10; 10**	**5**	2012	500	+0.96	+0.25	+0.71	+0.31
3	FGOALS-g2	5; 1	—	—	840	—	—	—	—
4	FIO-ESM	3; 3	—	—	800	+1.06	—	—	+0.21
5	**GFDL-CM3**	**5; 3**	**3**	2005	5200	+1.05	+0.16	+0.89	+0.22
6	GFDL-ESM2G	1; 1	—	—	500	—	—	—	—
7	GFDL-ESM2M	1; 1	1	2005	500	—	—	—	—
8	GISS-E2-H-CC	1; 1	—	—	251	—	—	—	—
9	**GISS-E2-H**	**5; 2**	**5**	2012	240	+1.20	+0.15	+1.05	+0.08
0	GISS-E2-R-CC	1; 1	—	—	251	—	—	—	—
1	**GISS-E2-R**	**6; 2**	**5**	2012	550	+1.03	+0.16	+0.87	+0.25
2	HadGEM2-AO	1; 1	—	—	700	—	—	—	—
3	HadGEM2-CC	1; 1	—	—	240	—	—	—	—
4	HadGEM2-ES	4; 4	1	2012	574	+1.24	—	—	+0.03
5	inmcm4	1; 1	—	—	500	—	—	—	—
6	**IPSL-CM5A-LR**	**5; 4**	**3**	2012	1000	+1.62	+0.19	+1.43	−0.35
7	IPSL-CM5A-MR	3; 1	3	2012	300	—	—	—	—
8	IPSL-CM5B-LR	1; 1	—	—	300	—	—	—	—
9	MIROC5 5; 3	—	—	—	670	+0.60	—	—	+0.68
0	MIROC-ESM-CHEM	1; 1	1	2005	255	—	—	—	—
1	MIROC-ESM	3; 1	1	2005	630	—	—	—	—
2	MPI-ESM-LR	3; 3	—	—	1000	+1.42	—	—	−0.14

ID	Model Name	# Runs: All-Forcing; RCP8.5 extension	# Runs: Natural Forcing	End Year: Natural Forcing	# Years: Control Run	All-Forcing Ens. Mean, °C	Natural Forcing Ens. Mean, °C	Anthro. Forcing Ens. Mean, °C	Internal Variab. Residual Est., °C
3	MPI-ESM-MR	3; 1	—	—	1000	—	—	—	—
4	MRI-CGCM3	3; 1	1	2005	500	—	—	—	—
5	NorESM1-ME	1; 1	—	—	252	—	—	—	—
6	NorESM1-M	3; 1	1	2012	501	—	—	—	—

(http://www.ncdc.noaa.gov/monitoring-references/faq/anomalies.php; Karl et al. 2015). Model data in main text Fig. 3.1 use surface air temperature over land points and sea surface temperature over ocean points except for ice-covered ocean points, where the surface temperature of the ice is used. Model data are masked according to the availability of observations in GISTEMP. Global mean anomalies are computed as the average of the Northern and Southern Hemisphere means for models and observations, except for the NOAA timeseries. Model anomalies are created using the model's masked 1951–80 climatology, and all series are shifted to have zero mean for 1881–1920. The Natural Forcing response curve uses 18 (10) models for 1880–2005 (2006–12).

S.3. Monthly observed internal variability maps for 2016.

Monthly maps of observed surface temperature internal climate variability anomalies for 2016 (Fig. ES3.1) were estimated by subtracting the CMIP5 All-Forcing response from observations. These indicate that for the 2015–16 El Niño event, warm anomalies in the equatorial Pacific lasted through April 2016, but were already replaced by pronounced cool equatorial Pacific anomalies by July 2016 and for the remainder of 2016 (Hu and Fedorov 2017). Global temperature anomalies peaked in February and March 2016, due to fading equatorial Pacific warmth combined with lingering warmth in parts of the tropical oceans and strong, extensive warm anomalies over Northern Hemisphere continents. The warm anomalies outside of the equatorial Pacific were partly a lagged response to El Niño (Trenberth et al. 2002; L'Heureux et al. 2017), as global temperature anomalies typically lag El Niño by about three months. The very pronounced warm anomalies seen over Asia during December 2015–April 2016, however, are not a typical lagged feature of El Niño in these studies. In summary, we infer from these results and the previous findings of Trenberth et al. (2002), L'Heureux et al. (2017), and Hu and Fedorov (2017), that the short-term global mean warmth in 2015 and 2016 is likely to have been at least partly El Niño-driven. Further studies would be needed to quantify El Niño's contribution to 2016 global temperatures with more confidence.

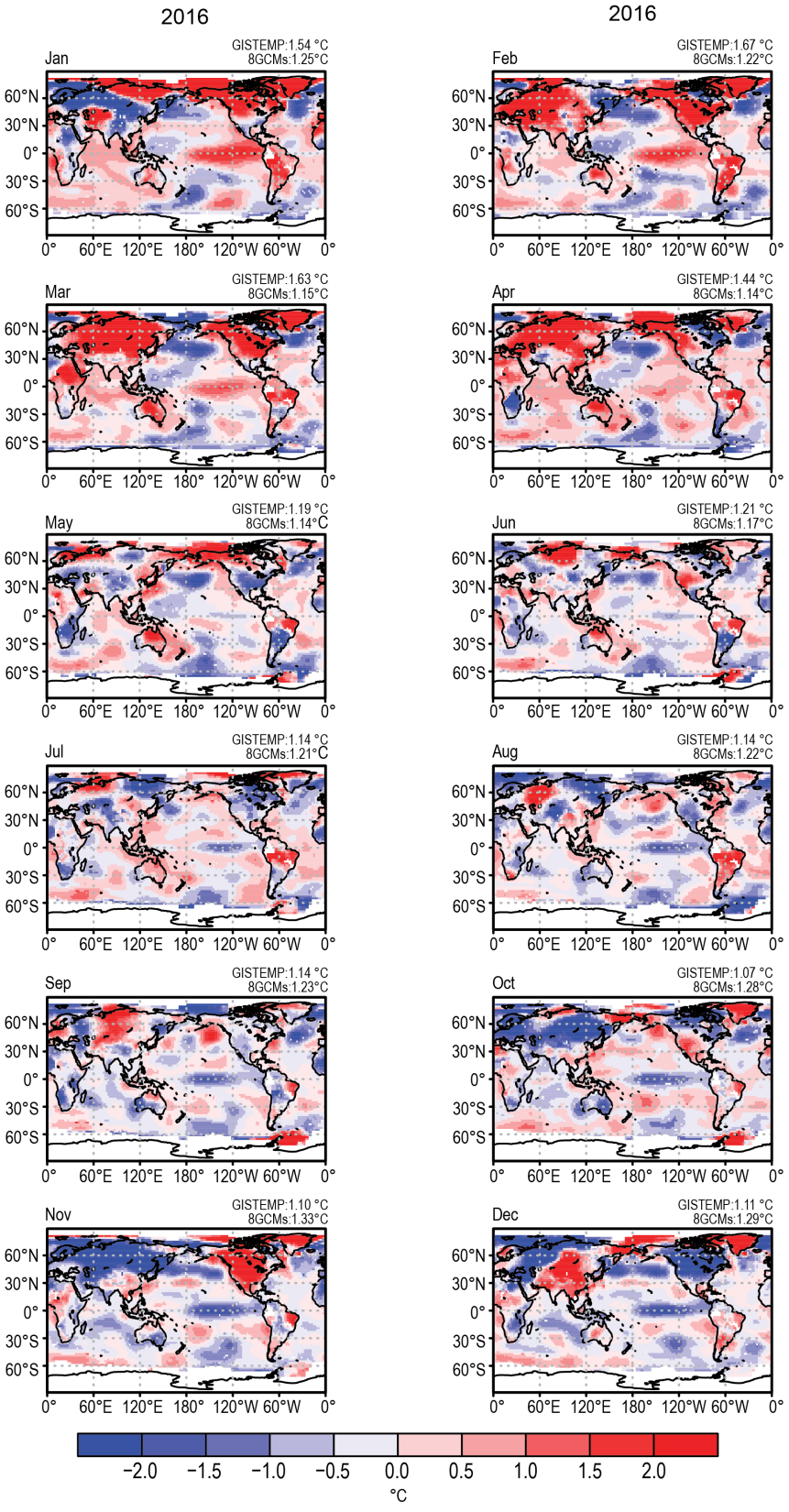

Fig. ES3.1. Monthly maps of 2016 GISTEMP surface temperature deviations from the CMIP5 All-Forcing anomalies(°C; 1880–1920 base period). The global average anomalies of GISTEMP and the CMIP5 8-model mean from the 1881–1920 base period are in the title line above each panel. The 8 models used include: CanESM2, CESM1-CAM5, CSIRO-Mk3-6-0, GFDL-CM3, GISS-E2-H, GISS-E2-R, IPSL-CM5A-LR, and IPSL-CM5A-LR.

REFERENCES

Hansen, J., R. Ruedy, M. Sato, and K. Lo, 2010: Global surface temperature change. *Rev. Geophys.*, **48**, RG4004, doi:10.1029/2010RG000345.

Hu, S., and A. V. Fedorov, 2017: The extreme El Niño of 2015-2016 and the end of global warming hiatus. *Geophys. Res. Lett.*, **44**, 3816–3824, doi:10.1002/2017GL072908.

IPCC, 2013: Climate Change 2013: *The Physical Science Basis. Contribution of Working Group I to the Fifth Assessment Report of the Intergovernmental Panel on Climate Change*. T. F. Stocker et al., Eds., Cambridge University Press, 1535 pp.

Karl, T. R., and Coauthors, 2015: Possible artifacts of data biases in the recent global surface warming hiatus. *Science*, **348**, 1469–1472, doi:10.1126/science.aaa5632.

Knutson, T. R., F. Zeng, and A. T. Wittenberg, 2013: Multimodel assessment of regional surface temperature trends: CMIP3 and CMIP5 twentieth-century simulations. *J. Climate*, **26**, 8709–8743, doi:10.1175/JCLI-D-12-00567.1.

Knutson, T. R., R. Zhang, and L. W. Horowitz, 2016: Prospects for a prolonged slowdown in global warming in the early 21st century. *Nat. Comm.*, **7**, 13676, doi:10.1038/ncomms13676.

L'Heureux, M., and Coauthors, 2017: Observing and predicting the 2015–16 El Niño. *Bull. Amer. Meteor. Soc.*, **98**, 1363–1382, doi:10.1175/BAMS-D-16-0009.1.

Morice, C. P., J. J. Kennedy, N. A. Rayner, and P. D. Jones, 2012: Quantifying uncertainties in global and regional temperature change using an ensemble of observational estimates: The HadCRUT4 data set. *J. Geophys. Res.*, **117**, D08101, doi:10.1029/2011JD017187.

Ridley, D. A., and Coauthors, 2014: Total volcanic stratospheric aerosol optical depths and implications for global climate change. *Geophys. Res. Lett.*, **41**, 7763–7769, doi:10.1002/2014GL061541.

Taylor, K. E., R. J. Stouffer, and G. A. Meehl, 2012: An overview of CMIP5 and the experimental design. *Bull. Amer. Meteor. Soc.*, **93**, 485–498, doi:10.1175/BAMS-D-00094.1.

Trenberth, K. E., J. M. Caron, D. P. Stepaniak, and S. Worley, 2002: Evolution of El Niño–Southern Oscillation and global atmospheric surface temperatures. *J. Atmos. Res.*, **107**, 4065, doi:10.1029/2000JD000298.